Uncertainties in fertilizer-induced emissions of soil nitrogen oxide and the associated impacts on ground-level ozone and methane

- Cheng Gong^{1*}, Yan Wang², Hanqin Tian^{3,4}, Sian Kou-Giesbrecht⁵, Nicolas Vuichard⁶ and Sönke Zaehle¹
- 5 Max Planck Institute for Biogeochemistry, Jena, 07745, Germany
- 6 ² State Key Laboratory of Subtropical Silviculture, College of Environment and Resources, College of
- 7 Carbon Neutrality, Zhejiang A&F University, Hangzhou, 311300, China
- 8 ³Center for Earth System Science and Global Sustainability, Schiller Institute for Integrated Science
- 9 and Society, Boston College, Chestnut Hill, MA, USA
- ⁴Department of Earth and Environmental Sciences, Boston College, Chestnut Hill, MA, USA
- ⁵Simon Fraser University, Canada
- ⁶Laboratoire des Sciences du Climat et de l'Environnement, LSCE-IPSL (CEA-CNRS-UVSQ),
- 13 Université Paris-Saclay, Gif-sur-Yvette, France

14 15

Abstract

- Natural and agricultural soils are important sources of nitrogen oxides (NO_x), accounting for about 10%
- 17 20% of the global NO_x emissions. The increased application of nitrogen (N) fertilizer in agriculture
- has strongly enhanced the N availability of soils in the last several decades, leading to higher soil NO_x
- 19 emissions. However, the magnitude of the N fertilizer-induced soil NO_x emissions remains poorly
- 20 constrained due to limited field observations, resulting in divergent estimates. Here we integrate the
- 21 results from meta-analyses of field manipulation experiments, emission inventories, atmospheric
- 22 chemistry modelling and terrestrial biosphere modelling to investigate these uncertainties and the
- associated impacts on ground-level ozone and methane. The estimated present-day global soil NO_x
- 24 emissions induced by N fertilizer application varies substantially (0.84–2.2 Tg N yr⁻¹) among different
- approaches with different spatial patterns. Simulations with the 3-D global chemical transport model
- 26 GEOS-Chem demonstrate that N fertilization enhances global surface ozone concentrations during
- 27 summertime in agricultural hotspots, such as North America, western Europe and eastern and southern
- Asia by 0.1 to 3.3 ppbv (0.2% 7.0%). Our results show that such spreads in soil NO_x emissions also
- affect atmospheric methane concentrations, reducing the global mean by 6.7 (0.4%) ppbv to 16.6 (0.9%)
- 30 ppbv as indirect consequence of enhanced N fertilizer application. These results highlight the urgent
- 31 need to improve the predictive understanding of soil NO_x emission responses to fertilizer N inputs and
- 32 its representation in atmospheric chemistry modelling.

33

34

*Correspondence to: Cheng Gong (cgong@bgc-jena.mpg.de)

1. Introduction

- 36 Nitrogen oxides (NO_x=NO + NO₂), as one of the most important reactive atmospheric components,
- 37 strongly affect the atmospheric oxidation capacity and further influence air quality (Gong et al., 2020;
- Zhai et al., 2021; Goldberg et al., 2022; Zhao et al., 2023), radiative forcing (Erisman et al., 2011; Pinder
- et al., 2012; Gong et al., 2024), as well as carbon (C) storage in terrestrial and marine ecosystems
- 40 (Fowler et al., 2013; Fleischer et al., 2019; Rubin et al., 2023). The major source of present-day
- 41 atmospheric NO_x is fossil fuel combustion (Martin et al., 2003; Hoesly et al., 2018), but several non-
- 42 fossil-fuel sources, including emissions from soils, lightning and wildfire (Zhang et al., 2003),
- contribute to around 30% of the global total NO_x emissions (Delmas et al., 1997; Weng et al., 2020).
- 44 However, these non-fossil-fuel sources have been widely regarded as 'natural' sources, where the
- 45 perturbation by anthropogenic activities as well as the associated potentially significant effects on the
- 46 N cycle are often overlooked. Meanwhile, strict clean-air actions have been applied in many countries
- 47 in the past decades to sharply reduce the fossil-fuel sources of NO_x (Jiang et al., 2022). As a result, non-
- 48 fossil sources of NO_x will be increasingly important for future clean air policies.
- 49 One of the most important non-fossil-fuel anthropogenic sources of NO_x is through agricultural
- activities, which have been estimated to enhance soil NO_x emissions by around 5%- 30% (Wang et al.,
- 51 2022; Gong et al., 2024). To assess the soil NO_x emissions induced by N fertilizer application (hereafter,
- 52 SNO_x-Fer), the most straightforward and widely-used method is applying the emission factor (EF),
- which indicates the proportion of N from fertilizer application emitted as NO_x. The Intergovernmental
- Panel on Climate Change (IPCC) methodology recommended a constant EF value 1.1% with an
- uncertainty range of 0.06% to 2.18% (Hergoualc'h et al., 2019). Other studies recommend slightly
- 56 smaller uncertainty ranges (0.47% to 1.61%) based on different meta-analysis datasets (Stehfest and
- 57 Bouwman, 2006; Liu et al., 2017; Skiba et al., 2021; Wang et al., 2022). This large uncertainty range
- results from the dependency of the response of soil NO_x emissions on intricate soil biogeochemical
- 59 processes and varies with crop types, soil texture, fertilizer types and application rate (Wang et al.,
- 60 2022). To date, limited field experiments are available to constrain this uncertainty range.
- Some studies have suggested to use non-linear EF to take account of the observations that the EFs of
- 62 soil reactive nitrogen gases tend to increase with increasing fertilizer application (Shcherbak et al., 2014;
- 63 Jiang et al., 2017). Such approach assumes that plants and soil microbes should have priority to access
- 64 soil available N for their metabolic activities, while the excessive inorganic N can be used by nitrifiers
- and denitrifiers and loses as the gas form. Such a non-linear EF approach is more ecologically
- 66 reasonable but there remain large uncertainties in assessing soil NO_x due to the limited available field
- data. For example, Wang et al. (2024) examined the non-linear EF of soil NO_x based on a global meta-
- analysis and found a much lower EF (around 0-0.7%) than the IPCC recommended linear EF (1.1%)
- 69 within the range of normal agricultural crop N fertilizer loading (around 0-600 kg N ha⁻¹ yr⁻¹).

In many of the atmospheric chemical transport model (CTMs), SNO_x-Fer is represented by the agriculture sector of NO_x emission from an anthropogenic emission inventory (e.g. Emissions Database for Global Atmospheric Research (EDGAR) or Community Emissions Data System (CEDS)), which in general apply the method of linear EF to estimate the agricultural NO_x emissions (Hoesly et al., 2018; Janssens-Maenhout et al., 2019; Nicholas Hutchings et al., 2023) with the caveats described above. Furthermore, some advanced CTMs, e.g. the GEOS-Chem model, parametrizes soil NO_x emissions as a function of N availability as well as soil temperature and soil moisture (Steinkamp and Lawrence, 2011; Hudman et al., 2012). The currently widely-used soil NO_x scheme named by the Berkeley-Dalhousie Soil NO_x Parameterization (BDSNP) could dynamically simulate the spatiotemporal variations of soil NO_x emissions, however, the responses of soil NO_x to N fertilizer application are not fully examined (See the detailed parameterization in Sect. 2)..

Recently, another approach to modelling SNO_x-Fer has emerged by the development of global, process-based terrestrial biosphere models (TBMs) with fully-coupled C and N cycles (Zaehle and Friend, 2010; Tian et al., 2019). Driven by data of N inputs (N synthesis fertilizer, N manure application and N deposition), CO₂ concentrations and climate, these TBMs could simulate the coupled-cycles of C and N in the terrestrial biosphere, mimic the competition on the available N between plants and microbes and calculate the rates of nitrification and denitrification (Zaehle and Dalmonech, 2011), which are the two microbial processes that determine the rates of soil NO_x emissions. Even though TBMs provides a more ecologically-mechanistic description of the terrestrial N cycles, large uncertainties remained among different TBMs due to the varying parameterization and modelling schemes on biome N use strategies, mineralization of organic N, nitrification and denitrification processes (Kou-Giesbrecht et al., 2023), which lead to varied responses of soil NO_x to the increased N fertilizer inputs (Gong et al., 2024).

In this study, we attempt to comprehensively quantify the uncertainties in current SNO_x-Fer estimates by integrating results from meta-analyses, emission inventories, as well as CTMs and TBMs. We use this understanding to assess the associated effects of SNO_x-Fer uncertainties on global O₃ and CH₄ concentrations. Section 2 will introduce the N synthetic fertilizer and manure input data and each approach to estimate SNO_x-Fer. Section 3 will introduce the CTM model used in this study and the configuration of sensitive experiments. Section 4 will firstly show the variations of SNO_x-Fer among different approaches as well as the seasonal dynamics, and then analyze the associated uncertainties in global O₃ and CH₄ simulations. Finally, the conclusion and discussions of this study will be given in section 5.

2. Data and Methods

2.1. Linear and Non-linear EFs and the global fertilizer N dataset

- We firstly implement the most traditional method with a constant EF value to estimate the effects of N
- fertilizer application on soil NO_x emissions, where the value of 1.1% (1.1% of N in the fertilizer will
- be emitted as NO_x ; named as EF_{linear} hereafter) based on the most up-to-date IPCC methodology is
- adopted (Hergoualc'h et al., 2019). Furthermore, based on the latest meta-analysis dataset developed by
- Wang et al. (2024), a non-linear EF method ($EF_{non-linear}$) to describe the variations of soil NO_x emissions
- with different N fertilizer loadings is also applied:

$$EF_{non-lineg} = (0.22 + 0.008 \times Fertilizer_N) \tag{1}$$

- where the $EF_{non-linear}$ (%) is the non-linear EF and $Fertilizer_N$ is the loading of fertilizer N application
- (kg N ha⁻¹). The detailed derivation of this formula is presented by in Wang et al. (2024), which follows
- a comparable method as presented by Shcherbak et al. (2014).
- We used the dataset of History of anthropogenic Nitrogen inputs (HaNi) (Tian et al., 2022) for the
- global rate of synthetic fertilizer and manure application, in order to estimate SNO_x-Fer with both of
- the linear and non-linear EF methods. The HaNi dataset includes grid-level annual loadings of (1) NH₄⁺-
- N synthetic fertilizer applied to cropland, (2) NO₃-N synthetic fertilizer applied to cropland, (3) NH₄+
- N synthetic fertilizer applied to pasture, (4) NO₃-N synthetic fertilizer applied to pasture, (5) manure
- 120 NH₄⁺-N application on cropland, (6) manure NO₃⁻-N application on pasture, (7) manure NH₄⁺-N
- deposition on pasture, (8) manure NO₃-N deposition on rangeland. We use a global map of land use
- class distributions (Hurtt et al., 2020) (Fig. S1) to convert the unit of N loading in HaNi from g N grid
- 123 to kg N (ha pasture)⁻¹, kg N (ha rangeland)⁻¹ or kg N (ha cropland⁻¹). The annual N inputs from HaNi
- dataset, which are summed by all N forms of synthetic fertilizer and manure, are evenly applied in the
- months of growing season, while the rates of N inputs are set as zero during the non-growing season.
- We define growing season as monthly-mean 2-metre temperature larger than 5 degree Celsius (based
- on the MERRA2 reanalyzed dataset, see below Sect. 3) and the grid-level monthly-mean leaf area index
- 128 (LAI) larger than 0.5 (based on MODIS remote sensing dataset postprocessed by Yuan et al. (2011) and
- 129 updated for the use of GEOS-Chem,
- 130 http://geoschemdata.wustl.edu/ExtData/HEMCO/Yuan_XLAI/v2021-06/). Finally, the rates of
- synthetic fertilizer and manure N inputs with the unit of kg N (ha pasture/rangeland/cropland)⁻¹ month
- ¹ are utilized to estimate global SNO_x-Fer with the both of the linear and non-linear EF approaches (Fig.
- 133 S2).
- 134 2.2. The emissions inventory CEDS
- We use the CEDS (Hoesly et al., 2018) for assessing the fertilizer-induced soil NO_x emissions in the
- emission inventories. CEDS is one of the most state-of-art emission inventories that comprehensively
- assess the sources of dominant air pollutants from pre-industrial period to present days, which has been
- used as the standard emission inventory to drive CMIP6 models. The agricultural NO_x emissions in

- 139 CEDS is from the EDGAR 4.3.1 (https://edgar.jrc.ec.europa.eu/), where the old IPCC methodology
- (Eggleston et al., 2006) is used with a constant EF value of 0.7% (0.7% of N in the fertilizer will be
- emitted as NO_x) (Janssens-Maenhout et al., 2019).
- 142 2.3. The BDSNP scheme
- The BDSNP scheme in CTMs is firstly developed by Yienger and Levy (1995), and then updated by
- Hudman et al. (2012). The emission of soil NO_x (S_{nox}) is described as:

145
$$S_{nox} = (A_{w \ biome} + N_{avail} \times \bar{E}) \times f(T) \times g(\theta) \times P(l_{drv})$$
 (2)

- Where f(T), $g(\theta)$ and $P(l_{dry})$ indicate the effects of temperature, soil moisture and the rain pulsing.
- 147 $A_{w,biome}$ is the wet biome-dependent emission (the baseline emission) from Steinkamp and Lawrence
- 148 (2011). N_{avail} is the soil available N mass in the top 10 cm (ng N m⁻²), which is calculated by:

149
$$N_{avail}(t) = N_{avail}(0)e^{-\frac{t}{\tau}} + Fertilizer_N \times \tau \times (1 - e^{-\frac{t}{\tau}})$$
 (3)

- Where the initial soil available N mass $N_{avail}(0)$ is prescribed. Fertilizer_N is the rate of fertilizer N
- application, which is set as zero outside the growing season. τ indicates the decay rate and is chosen as
- 4 months based on the measurement within the top 10 cm soil (Matson et al., 1998; Cheng et al., 2004;
- Russell et al., 2011). However, it should be noted that magnitude of global SNO_x-Fer (i.e. the $N_{avail} \times \bar{E}$)
- is scaled by the factor \bar{E} in Eq. (2) to meet 1.8 Tg N yr⁻¹ before the canopy reduction, which is the value
- obtained in a previous meta-analysis study based on the fertilizer N input dataset in 2000s (Stehfest and
- Bouwman, 2006). As a result, the default BDSNP scheme in GEOS-Chem actually fails to capture the
- year-to-year variations of soil NO_x emissions with the changing soil N availability. However, as the
- BDSNP scheme is still widely used by the community of atmospheric chemistry modelling (e.g. Lu et
- al., 2021; Wang et al., 2022; Huber et al., 2023), here we add another sensitivity experiment by scaling
- the N_{avail} in Eq.3 following the interannual variations of the HaNi fertilizer loadings:

161
$$N_{avail}(i,j,yr) = N_{avail}(i,j,2000) * \frac{Fertilizer_{HaNi}(i,j,yr)}{Fertilizer_{HaNi}(i,j,2000)}$$
(4)

- Where $Fertilizer_{HaNi}(i, j, yr)$ represents the total N fertilizer loadings in HaNi dataset at the grid of i
- latitude and j longitude in the yr year. With this modification, we could further examine how SNO_x-Fer
- responses to the N fertilizer enhancement in the GEOS-Chem BDSNP scheme.
- 165 2.4. The TBM ensemble
- 166 Simulated soil NO_x emissions were provided by three TBMs (CLASSIC, OCN and ORCHIDEE) with
- fully-coupled C and N cycles included in the global nitrogen/N₂O model inter-comparison project phase
- 2 (NMIP2) (Tian et al., 2024). For each TBM model, anthropogenic fertilizer application are estimated
- by the HaNi dataset (Tian et al., 2022), where the fertilizer types (NH₄⁺ and NO₃⁻; synthetic fertilizer

and manure) are explicitly distinguished in the model. The SNO_x-Fer can be isolated by summing up the differences between sensitivity experiments SH1 and SH2 (the synthetic fertilizer contribution) and the differences between sensitivity experiments SH1 and SH3 (the manure contribution) (Table S1). It should be noted that the CLASSIC model did not isolate synthetic fertilizer and manure and thus only conducted one sensitivity experiment. The model ensemble mean is utilized to smooth the large discrepancies among different TBMs (Fig. S3) due to the varied terrestrial N-cycle representations, in particular, the varied nitrification and denitrification rates.

3. The GEOS-Chem model and sensitivity experiment configuration

The GEOS-Chem model is a frequently used state-of-the-art CTMs with fully coupled NOx–Ox–hydrocarbon–aerosol chemistry mechanism (Bey et al., 2001; Park et al., 2004). Here we applied the version 12.0.0 to run the global simulation with a horizontal resolution of 2° latitude × 2.5° longitude. The simulations are driven by the Version two of modern era retrospective-analysis for research and application (MERRA2) reanalyzed meteorological dataset. The photolysis rates were computed by Fast-JX scheme (Park et al., 2004). The atmospheric gas-phase chemistry is independently developed referring to the kinetics and products based on JPL recommendations (Bates et al., 2024) and solved by the Kinetic Pre-Processor (KPP) (Henze et al., 2007). Aerosol thermodynamic equilibrium is calculated by the ISORROPIA II package (Fountoukis and Nenes, 2007). In particular, the default soil NO_x emissions are simulated by the BDSNP scheme as introduced above.

In order to examine the uncertainties in the SNO_x-Fer and the associated effects on global surface O₃ concentrations, we firstly run a reference simulation in 2019 (named Zero) with zero SNO_x-Fer to exclude the influence of fertilizer application on soil NO_x. Then eleven different experiments are performed by representing SNO_x-Fer with CEDS agricultural NO_x emissions (named CEDS), the default GEOS-Chem BDSNP scheme (Eqs. 2-3, named BDSNP_coarse), the BDSNP scaled by the interannually-varied HaNi N fertilizer loadings (Eq. 4, named BDSNP_coarse_scaled), the default GEOS-Chem BDSNP but with fine resolution of 0.5°×0.625° (named BDSNP_fine), the TBM-simulated SNO_x-Fer of each model as well as the ensemble mean (named NMIP2-OCN, NMIP2-CLASSIC, NMIP2-ORCHIDEE and NMIP2, respectively), the linear EF (EF=1.1%) method (named Linear) and the non-linear EF (Eq. 1) method (named Nonlinear), respectively. In particular, the BDSNP_fine is simulated offline, i.e. the atmospheric chemical and transport processes are not accounted due to the inconsistence of resolutions with the GEOS-Chem runs. All of the sensitivity experiments are driven by the meteorological field in the year of 2019 with 6-month spin up, where the anthropogenic emissions of all other tracers also keep at the level of 2019 following the CEDS inventory. Table 1 summarizes the eleven sensitivity experiments in GEOS-Chem.

In order to further examine the seasonality of SNO_x-Fer and the associated impacts on ground-level O₃ in agricultural hotspot regions, we investigate how different SNO_x-Fer approaches distribute the annual fertilizer seasonally (Table 1). The HaNi dataset, as well as the equivalently up-to-date fertilizer dataset (Adalibieke et al., 2023), only provide annual fertilizer application rates given the lack of specific information to distribute the N fertilization seasonally. The CEDS, BDSNP and NMIP2 models approaches have their own specific monthly distribution, while the monthly distribution of fertilizer application in the linear and nonlinear EF are arbitrarily assumed to be even during growing season. Here, we added two additional GEOS-Chem sensitivity experiments for the linear and non-linear approach, named Linear_7525 and Nonlinear_7525, which apply the seasonal pattern of the BDSNP scheme (Hudman et al., 2012), assuming that 75% of the annual fertilizer is applied in the first month of growing season and the rest 25% evenly applied in the rest growing months.

Table 1. Summary of the sensitivity experiments in GEOS-Chem and the methods used by different SNO_x-Fer estimating approaches to distribute the annual N fertilizer into monthly.

SNO _x -Fer estimating approch	Experimental name in this study	Emissions of SNO _x -Fer	Fertilizer monthly distribution	
None	Zero	Zero	None	
	Linear	Linear EF	Evenly distributed during the growing	
	Nonlinear	Nonlinear EF	season	
Emission Factor (EF)	Linear_7525 Nonlinear_7525	Linear EF Nonlinear EF	75% of the annual fertilizer is applied in the first month of growing season, while the rest 25% is evenly distributed in the rest	
Emission inventory	CEDS	CEDS agricultural NO _x sector	growing months Not clear	
	BDSNP_coarse	GEOS-Chem default BDSNP with resolution of 2°×2.5°	75% of the annual fertilizer is applied in	
BDSNP	BDSNP_coarse_scaled	BDSNP scaled with the interannual variations of HaNi fertilizer loadings with resolution 2°×2.5°	the first month of growing season, while the rest 25% is evenly distributed in the rest	
	BDSNP_fine (offline)	GEOS-Chem default BDSNP with resolution of 0.5°× 0.625°	growing months	

Terrestrial biosphere models (TBMs)	NMIP2-OCN	OCN simulated SNO _x -Fer	Distributed the annual N fertilizer loadings into four equal doses in the first half of the growing season	
	NMIP2-CLASSIC	CLASSIC simulated SNO _x -Fer	Evenly distributed throughout the year in the tropics (between 30S and 30N); Evenly distributed from spring equinox to fall equinox between 30N (30S) and 90N (90S)	
		NMIP2-ORCHIDEE	ORCHIDEE simulated SNO _x -Fer	Not clear
		NMIP2	TBMs ensemble mean	

Because the default GEOS-Chem simulations used above do not account for interactive CH₄ chemistry, we further conducted ten more sensitivity experiments with the special 'CH₄ run' in GEOS-Chem (East et al., 2024; Fu et al., 2024) to assess the variations in the atmospheric CH₄ concentrations induced by the uncertain SNO_x-Fer. The special CH₄ run takes CH₄ as the only one atmospheric transport tracer with various prescribed CH₄ sources (summarized in Table S2), while the CH₄ sinks include the tropospheric reactions with hydroxyl radical (OH) and chlorine, stratospheric loss and soil uptake. The global monthly mean OH concentrations archived from the ten sensitivity experiments (Table 1, except for the BDSNP_fine) are applied in the CH₄ simulation to assess the SNO_x-Fer effect on CH₄ lifetime through perturbing atmospheric oxidation capacity. As a result, there will be ten more associated sensitivity experiments with the CH₄ run that corresponds to the default GEOS-Chem simulations in Table 1 (except for the BDSNP_fine experiment). Each CH₄ simulation runs for 15 years by repeating the meteorological forcings in 2019 to reach a semi-equilibrium with the prescribed emissions and OH concentrations. The last year of the simulation is utilized to analyze the influences of soil NO_x on CH₄ induced by N fertilizer application. The simulated global surface CH₄ concentrations driven by varied OH levels from different sensitivity experiments are shown in Fig. S5.

- 236 4. Results
- 237 4.1 Varied SNO_x-Fer among different approaches
- Figure 1 shows the historical time series of global SNO_x-Fer over 1950-2019 estimated by different approaches, which is mainly driven by the substantial increases in global N fertilizer application.

 Almost all approaches except BDSNP showed enhancements in soil NO_x emissions but with largely

varied magnitudes from 0.6 to 2.1 Tg yr⁻¹ over 1950-2019. The default BDSNP scheme in GEOS-Chem, which scales soil NO_x emissions with time-variant temperature and soil moisture, but assumes constant N availability (see Methods), estimates the relatively stable soil NO_x emissions over 1980-2019. The annually-varied BDSNP scheme scaled by the HaNi N input dataset shows increase in SNO_x-Fer from 0.8 Tg N yr⁻¹ in 1980 to 1.5 Tg N yr⁻¹ in 2019, while the sharpest increase of the soil NO_x emission is simulated by the TBM ensemble, mainly induced by the high estimates of the CLASSIC and ORCHIDEE models (Fig. S3). Soil NO_x estimated by the non-linear EF approach shows substantially weaker response to fertilizer inputs relative to other estimating approaches.

Fertilizer-induced soil NO_x emissions

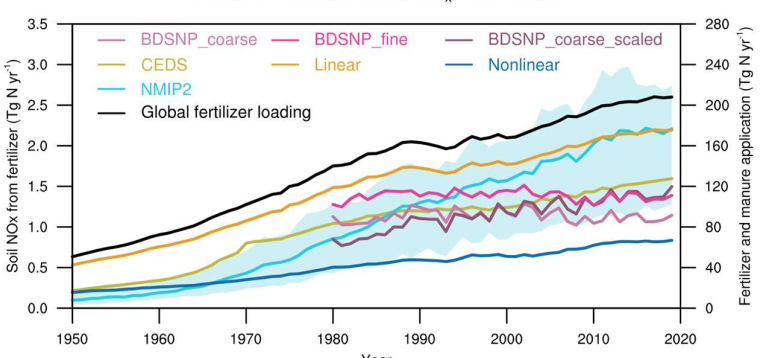


Figure 1. Global estimates of N fertilizer-induced soil NO_x emissions by different approaches. The black line (right Y axis) indicates global annual-mean N synthetic fertilizer and manure inputs over 1950-2019 assessed from the HaNi dataset. The rest lines (left Y axis) indicate the N fertilizer-induced soil NO_x emissions over 1950-2019 estimated by different approaches, including emission inventory (CEDS), linear and non-linear EF, the widely-used CTM parameterization with coarse resolution (2°×2.5°, BDSNP_corase), fine resolution (0.5°×0.625°, BDSNP_fine) and interannually varied N availability (BNDSP_corase_scaled), and the TBM ensembles (NMIP2). The light cyan shadows indicate the spread across three different TBMs in NMIP2.

Figure 3 shows the global spatial patterns of SNO_x-Fer among different approaches. Each approach shows consistent spatial patterns aligned with the distribution of N synthetic fertilizer and manure inputs (Fig. 2), where eastern U.S., western Europe, eastern and southern Asia are the hotspots with high soil NO_x emissions. Notably, even though the TBM ensemble (NMIP2) and the Linear EF approach estimate similar global total SNO_x-Fer, the spatial distributions of both estimates vary strongly. The SNO_x-Fer estimates by NMIP2 ensemble are higher in agricultural hotspots (Table 2), but lower in regions with less synthetic fertilizer application, e.g. in part of the Africa and South America (Figs. 3d and 3e), relative to the Linear EF approach. Because plants and microbes have high priority to assess additional N in N-limited regions, which leads less N loss as the gas forms. However, in N-saturated regions, the

applied N fertilizer excessive for the living biomes, yielding a higher sensitivity of soil NO_x emissions to N fertilizer application (Du and De Vries, 2025). Such N dynamics have been included in the C-N fully-coupled TBMs, but fail to be represented by the linear EF approach.'.

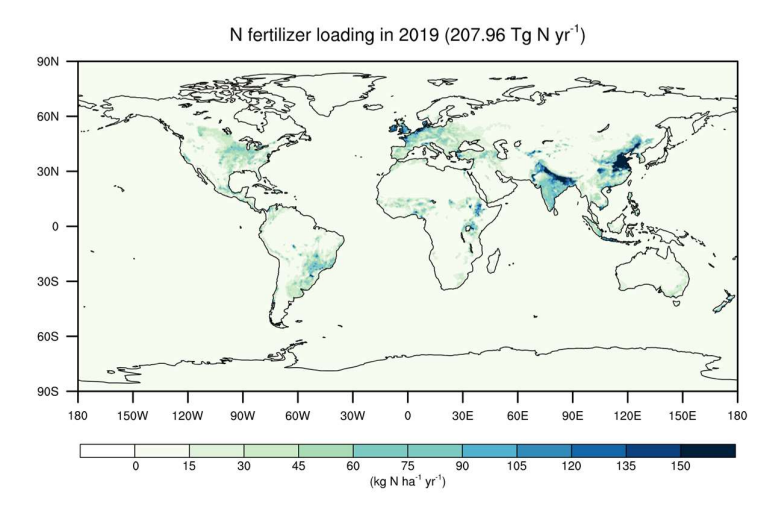


Figure 2. The global spatial patterns of N synthetic fertilizer and manure application in 2019 from the HaNi dataset.

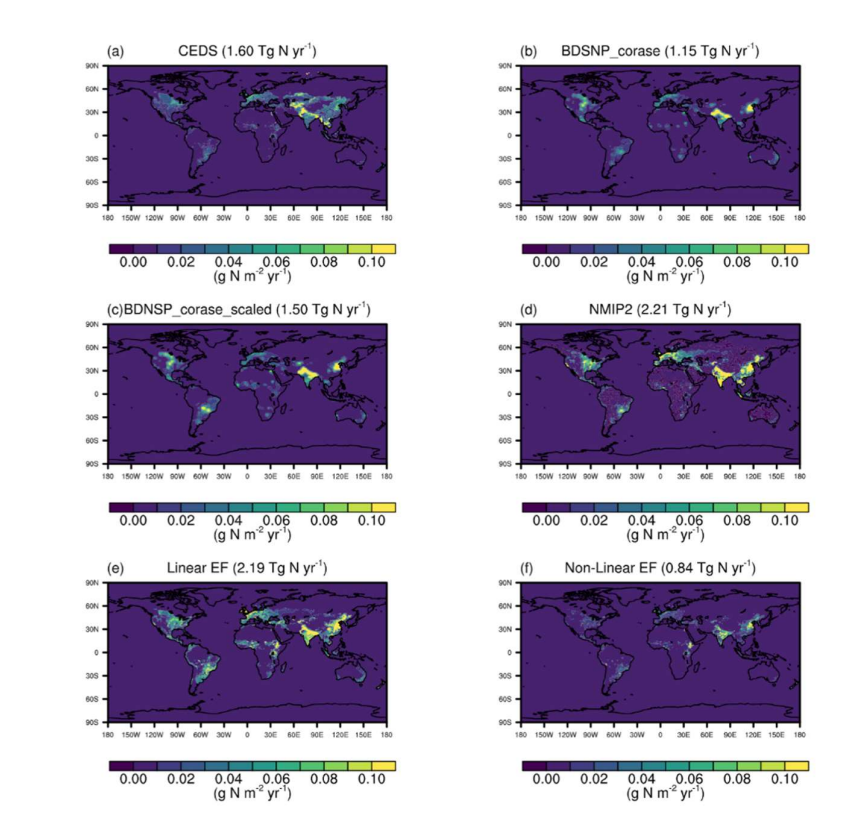


Figure 3. The N-fertilization induced soil NO_x emissions estimated by different approaches in 2019. (a) - (f) The soil NO_x emissions induced by N fertilizer estimated by the CEDS agricultural sector, the

default BDSNP scheme in GEOS-Chem with coarse resolution (2°×2.5°), the coarse-resolution BDSNP scheme in GEOS-Chem by interannually scaling the N availability using the HaNi dataset, the NMIP2 ensemble, the linear EF and non-linear EF, respectively. The global total budget of each estimate is given in the sub-titles.

Table 2. The annual soil NO_x emissions (Gg N yr⁻¹) induced by N fertilizer in 2019 in the eastern U.S., western Europe, eastern Asia, southern Asia as well as the global estimates by different approaches. The ranges in NMIP2 indicate the highest and lowest values among three TBMs (CLASSIC, ORCHIDEE and OCN)

	Eastern U.S.	Western Europe	Eastern Asia	Southern Asia	
	(35-45N, 75-	(35-60N, 10W-	(20-50N, 100-	(10-30N, 70-	Globe
	90W)	20E)	125E)	85E)	
CEDS	20.9	99.1	190.0	104.8	1600
BDSNP_corase	15.8	76.3	157.0	134.2	1150
BDSNP_corase_scaled	17.6	69.8	174.8	201.7	1500
NMIP2	57.0 [15.1, 100.9]	206.3 [67.4, 267.3]	417.5 [261.0, 598.1]	382.4 [78.4, 776.3]	2210 [1280, 2740]
Linear EF	54.3	181.0	376.4	214.7	2190
Non-Linear EF	15.6	60.8	136.5	141.8	840

4.2 The seasonal cycle of SNO_x-Fer and the associated impact on O₃ concentrations

Figure 4 shows the seasonality of SNO_x-Fer in four agricultural hotspot regions among different SNO_x-Fer estimating methods. In the temperate regions like Eastern U.S., Western Europe and Eastern Asia, the TBM ensembles NMIP2 shows very strong seasonal variations, which reaches highest during May to July in Eastern U.S., April to June in Western Europe and May to August in Eastern Asia, respectively. The seasonality of the linear and nonlinear EF methods is strongly dependent on the assumption of fertilizer applying time (Table 1), where the monthly SNO_x-Fer emissions are at similar levels during the growing season for the Linear and Nonlinear experiments, but peak in a pronounced manner in the north-hemispheric spring time (around February to April) in the Linear_7525 and Nonlinear_7525 cases. Although the BDSNP applies the same assumption of fertilizer applying time as Linear_7525 and Nonlinear_7525, the SNO_x-Fer in BDSNP peaks much later (September to October in Eastern U.S., June to August in Western Europe and May to June in Eastern Asia). This arises because the EF methods

estimate SNO_x-Fer instantaneously in response to the fertilizer application, but the BDSNP scheme cumulates N fertilizer with a 4-months time window (Eq. 3). It is also very important the BDSNP includes the regulation of soil temperature and moisture on SNO_x-Fer, both of which also have strong seasonality, but the EF methods do not. Furthermore, in the tropical regions of Southern Asia, the NMIP2, Linear_7525 and Nonlinear_7525 experiments estimate the peak SNO_x-Fer in the beginning of the year, while the SNO_x-Fer of BDSNP reaches highest in May due to the N cumulation assumption (Fig. 4d). The rest methods, including the emissions inventory CEDS, the Linear and Nonlinear EF method, show very weak seasonality of SNO_x-Fer in Southern Asia.

The seasonality of ground-level monthly MDA8 O₃ changes in response to the SNO_x-Fer in general aligns with the monthly variations of SNO_x-Fer among different estimating approaches (Fig. 5). The strongest enhancement of regional MDA8 O₃ shows during the north-hemispheric summertime (June-August) for most of the estimating approaches in three temperate regions, when the absolute O₃ concentrations also reaches highest. However, it should be noted that spring-peak SNO_x-Fer in the Linear_7525 and the Nonlinear_7525 cases does not lead to high O₃ enhancement in both Western Europe and Eastern Asia (Figs. 5b and 5c). The weak sensitivity of O₃ to NO_x during springtime is likely the result of the seasonal variations in other emissions (e.g. biogenic volatile organic compounds (BVOCs)), which alter the chemical sensitivity regime. The responses of O₃ to SNO_x-Fer could also depend on regions (e.g. O₃ enhancement also peaks during spring in Linear_7525 in Eastern U.S., Fig. 5a), spatial simulating resolution or different modelling chemical mechanisms. The O₃ enhancement in Southern Asia is generally similar during north-hemispheric spring and summer time for all of the SNO_x-Fer estimating approaches (Fig. 5d), except for the BDSNP scheme, which stimulates significantly higher O₃ enhancement during May to July relative to February to April.

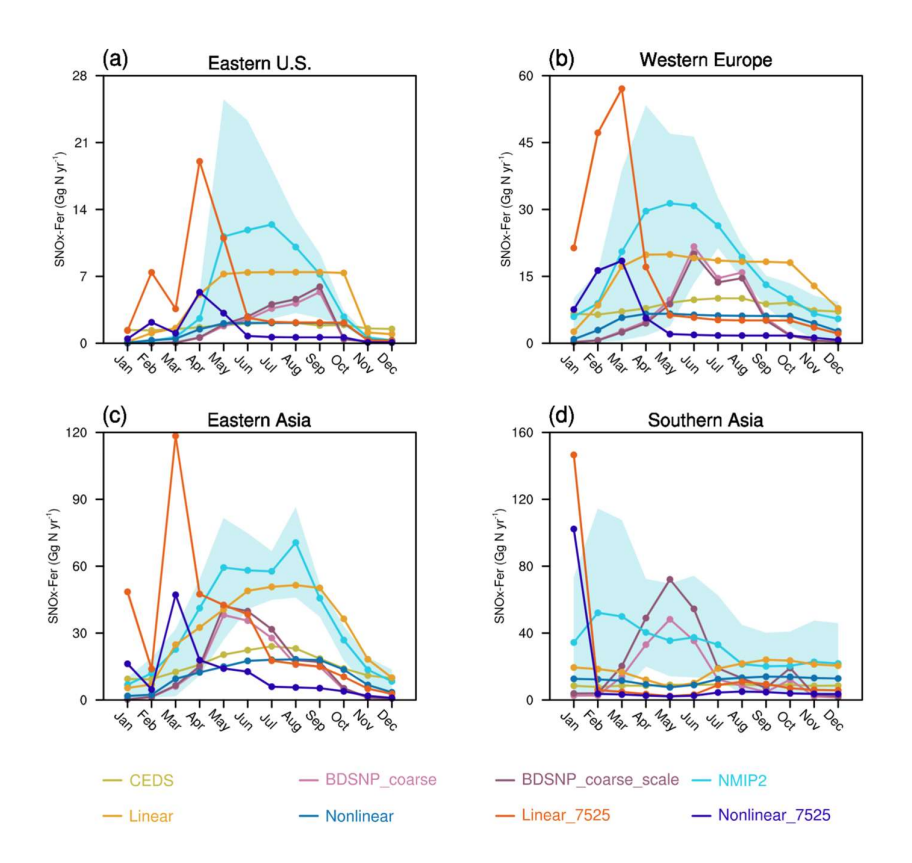


Figure 4. The monthly regional SNO_x-Fer (Gg N yr⁻¹) in the (a) Eastern U.S., (b) Western Europe, (c) Eastern Asia and (d) Southern Asia with different SNO_x-Fer estimating approaches. The cyan-blue shades indicate the spreads among three different TBM models (CLASSIC, OCN and ORCHIDEE) in the NMIP2 ensemble.

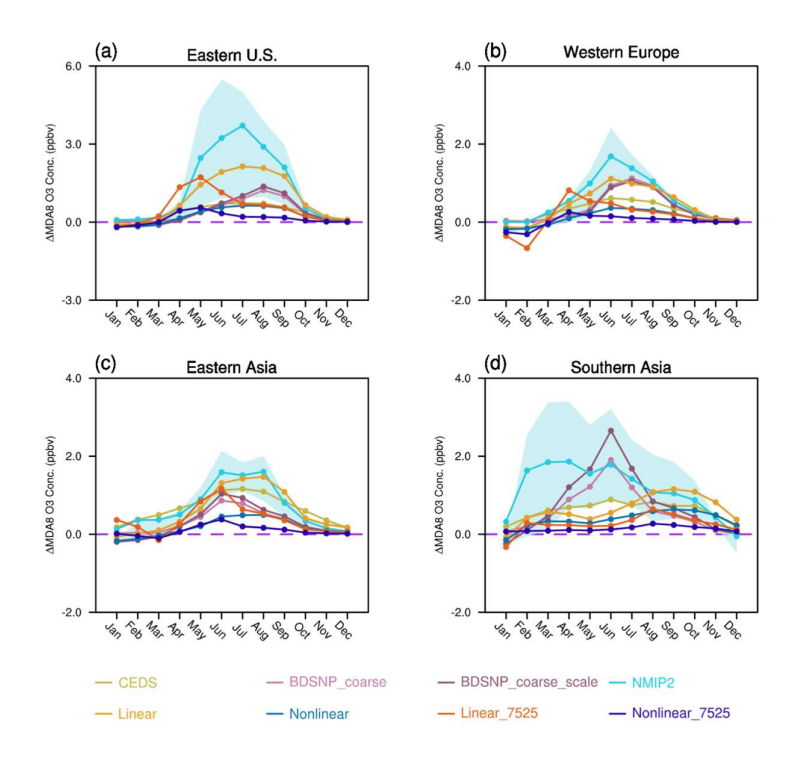


Figure 5. The regionally-averaged monthly MDA8 O₃ changes (ppbv) induced by SNO_x-Fer in the (a) Eastern U.S., (b) Western Europe, (c) Eastern Asia and (d) Southern Asia with different SNO_x-Fer estimating approaches. The cyan-blue shades indicate the spreads among three different TBM models (CLASSIC, OCN and ORCHIDEE) in the NMIP2 ensemble.

4.3 Impacts of SNO_x-Fer on surface O₃ concentrations

We next examine how the different SNO_x-Fer estimates influence the surface O₃ concentrations globally. Since soil NO_x emissions typically peak during the summer period (Fig. 5), when O₃ pollution tends to be most severe, we focus our analysis on the surface maximum daily 8-h averaged (MDA8) O₃ concentrations averaged over the northern hemisphere summer (June, July and August) based on the sensitivity experiments in Table 1. Figure 6 shows that the N fertilizer application enhanced the globally-averaged surface summertime O₃ MDA8 concentrations by 0.04-0.30 ppbv in 2019. In agricultural regions, the enhancement of O₃ concentrations due to SNO_x-Fer reaches 0.1-3.3 ppbv (0.2% - 7.0%) (Fig. 6). Figure 6 also highlights important differences in the spatial effect of NO_x on O₃, consistent with the regional effects on SNO_x-Fer (Table 2), that the NMIP2 estimate of SNO_x-Fer shows stronger contributions to the O₃ concentrations than the linear EF approach in agricultural regions. The non-linear EF method leads to the lowest O₃ enhancement, although both non-linear EF and TBMs estimates increasing soil NO_x emissions with soil N availability.

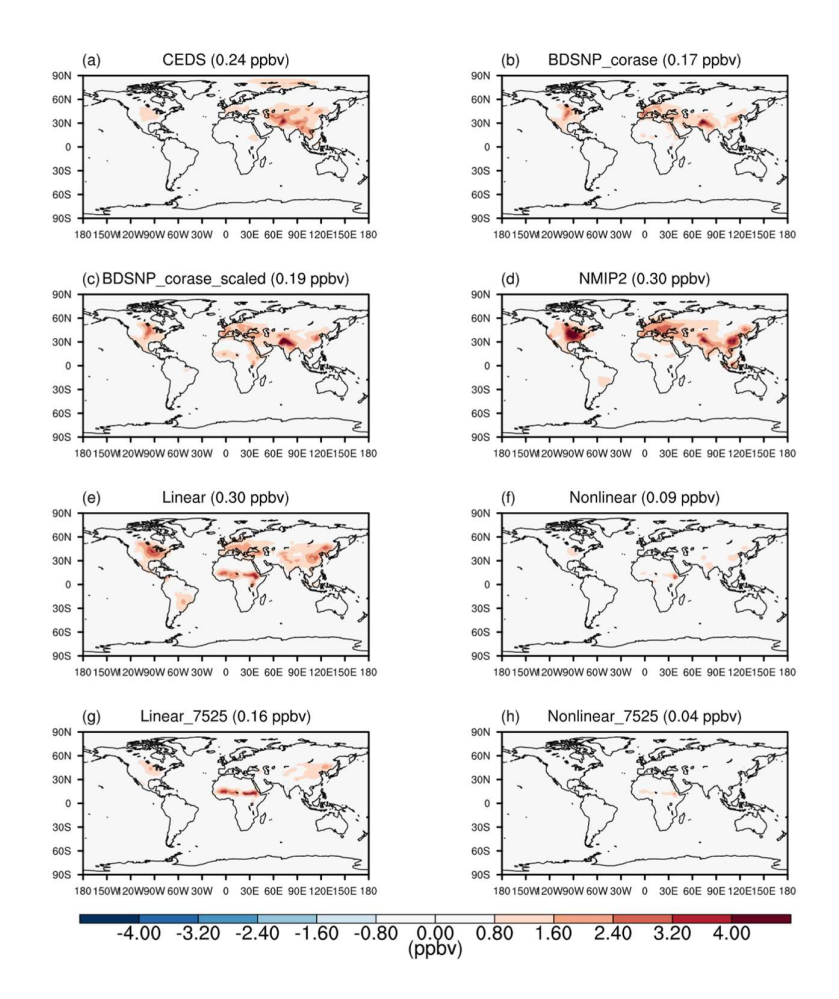


Figure 6. Global simulated changes in surface MDA8 O₃ concentrations induced by different estimating approaches of SNO_x-Fer averaged over June, July and August in 2019. The differences are calculated between corresponding sensitivity experiments in Table 1 and the Zero experiment. The numbers in each sub-title are changes in the global averaged summertime MDA8 O₃ concentrations induced by SNO_x-Fer.

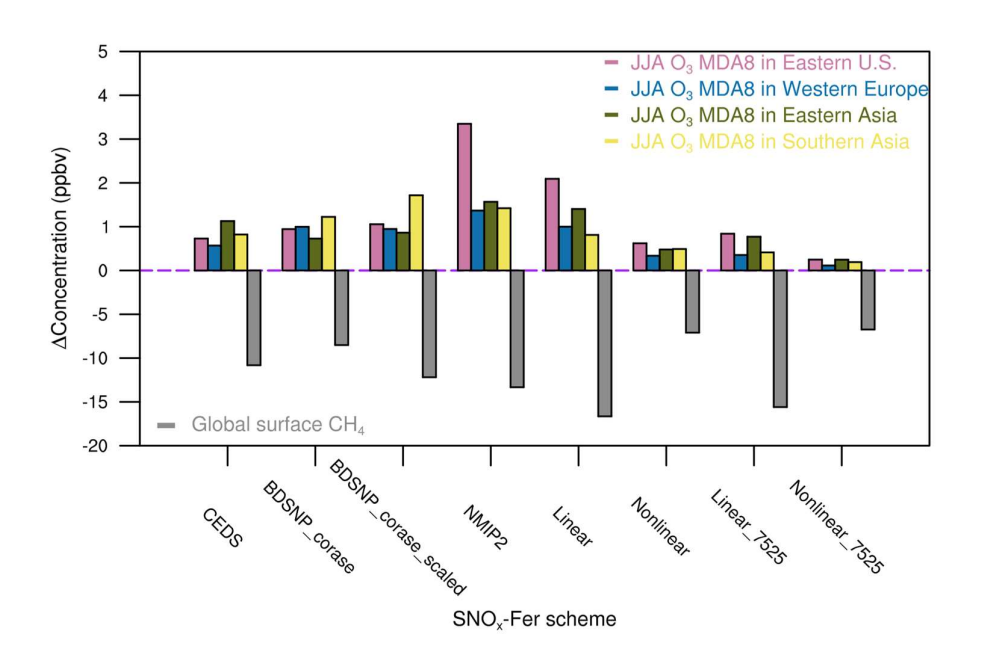


Figure 7. Changes in summertime averaged surface MDA8 O₃ concentrations (positive Y axis) and global surface CH₄ concentrations (negative Y axis) induced by SNO_x-Fer uncertainties. The regional MDA8 O₃ concentrations are averaged over Eastern U.S. (35-45N, 75-90W), Western Europe (35-60N, 10W-20E), Eastern Asia (20-50N, 100-125E) and Southern Asia (10-30N, 70-85E).

4.4 The impacts of SNO_x-Fer uncertainties on global CH₄ estimates

365 F
366 c
367 C
368 e
369 C
370 (J
371 m
372 w
373 e

Figure 7 shows that N fertilizer-induced soil NO_x induced the reduction of global averaged CH₄ concentrations ranging from 6.7 ppbv (0.4%) to 16.6 ppbv (0.9%) in 2019 by increasing atmospheric OH concentrations (Fig. S5), spatially aligned with the distributions of SNO_x-Fer among different estimating approaches (Fig. 3). Because CH₄ has a significantly longer atmospheric lifetime than either OH or NO_x, the spatial differences in the impacts of SNO_x-Fer on CH₄ concentrations are insignificant (Fig. S4). As a result, we only focus on the globally averaged changes in CH₄ concentrations. This magnitude of this estimate is consistent with recent estimates of around 17.4 ppbv by Gong et al. (2024), which relies on the same NMIP2 dataset and a simpler CH₄ box model to calculate the impacts of NO_x emissions on the atmospheric lifetime of CH₄. This result highlights an important but indirect role of SNO_x-Fer on atmospheric CH₄ concentrations, which is an often-overlooked aspect for the global CH₄ budget. However, the uncertainty range in our estimates clearly suggests the need to further improve our understanding in soil N biogeochemical processes to better predict global OH reactivity as well as close global CH₄ budget.

5. Discussions

In this study, we integrated knowledge from meta-analyses (Hergoualc'h et al., 2019; Wang et al., 2024), the emission inventory, parameterizations in CTMs and the TBM ensembles to better quantify the uncertainties in N fertilizer-induced soil NO_x emissions and the associated impacts on global O₃ and CH₄ concentrations. Our results showed a large variation of the global soil NO_x emissions associated with N fertilizer, ranging from 0.84 Tg N yr⁻¹ to 2.2 Tg N yr⁻¹ in 2019. This range of responses leads to an enhancement in summertime surface MDA8 O₃ concentrations of 0.1 ppbv to 3.3 ppbv (0.2%-7.0%) in agricultural hotspot regions. The O₃ enhancement is highest in eastern U.S., while it is not only determined by the SNO_x-Fer emissions, but also the diverging sensitivities of O₃ to NO_x depending on different chemical regime in GEOS-Chem (Fig. S6). The varied SNO_x-Fer estimates also lead to a reduction in global CH₄ concentrations of 6.7 ppbv (0.4%) to 16.6 ppbv (0.9%). These changes highlight a significant role of agricultural N use and soil N biogeochemical processes in affecting regional O₃ concentrations as well as controlling global greenhouse gases. In particular, with the worldwide reduction in fossil-fuel NO_x emissions associated with clean-air actions (Jiang et al., 2022), control of agricultural soil NO_x emissions becomes increasingly important to improve air quality and alleviate the associated public health risks.

However, challenges remain in the accurate assessment of N fertilizer-induced soil NO_x emissions. On the one hand, the overall uncertainties of SNO_x-Fer may still be underestimated. The EF-approach with fixed EF fails to adequately reflect the complexity in soil biogeochemical processes, which is reflected by the large ranges of EFs from 0.06% to 2.18% in a recent meta-analysis (Hergoualc'h et al., 2019). While the non-linear EF method represents an advance over the linear EF approach, as the effects of soil N saturation levels on soil N gas emissions are considered and therefore the approach yields relatively good performance in predicting soil N₂O or NH₃ emissions compared to observations (Shcherbak et al., 2014; Jiang et al., 2017), the limited availability of observations to constrain these responses and their limited spatiotemporal representativeness reduce the reliability of this approach. Most of the experimental data in Wang et al. (2024) are collected over China in the past ten years and thus may not be representative of other agricultural regions. Furthermore, 22 out of 55 data points are from vegetable cropping systems and orchard fields, where frequent irrigation may enhance soil moisture and thus inhibit the production of NO_x via nitrification. Last but not least, other factors, such as soil texture, pH, soil organic carbon and fertilizer types, may also affect the response of soil NO_x emissions to the loading of N fertilizer application, which are omitted by either the linear EF or nonlinear EF approach. As a result, more representative crop experiments with a gradient series of N addition are necessary to better constrain the soil NO_x response to N fertilizer application.

For the modelling of SNO_x-Fer, on the one hand, recent developments of the parameterization of BDSNP in CTMs focused more on the soil NO_x responses to changing temperature or soil moisture (e.g. Wang et al., 2021; Huber et al., 2023), while the accuracy of the soil N availability has been less

investigated. Even with the scaled N fertilizer loadings to interannually vary the N availability, BDSNP still showed weaker increasing trend of SNO_x-Fer in response to the N fertilizer enhancement relative to the empirical EF methods and the TBM simulations of NMIP2 in the past decades (Fig. 1). Nevertheless, it should be noted that the BDSNP scheme is also sensitive to the spatial resolution, where the coarse resolution may miss small-scale hotspots and thus underestimate the global SNO_x-Fer, as the BDSNP fine experiment shows in Fig. 1. On the other hand, terrestrial N availability is a key concept in the development of TBMs, as the process-based TBMs need detailed description of the N cycle to understand nutrient limitation levels and associated C-N coupling. Nevertheless, the soil NO_x emissions have been overlooked by the ecological modelling community because the low emissions may not be important for the terrestrial N cycle, resulting in a limited number of TBMs that include soil NO_x emissions as well as large inter-model variations (Fig. S2). To further reduce the uncertainties in soil NO_x emission estimates, the advantages of TBMs on representing soil N availability can be introduced into CTMs to better examine the effects of agricultural activities on atmospheric chemistry, but at the same time, the terrestrial N cycle needs to be further developed in TBMs to reduce inter-model variations and to better predict soil emissions of reactive N gases (not only NO_x but also N₂O and NH₃). The seasonality of SNO_x-Fer and the associated impacts on surface O₃ concentrations are also important but poorly constrained. The most difficult challenge is to precisely estimate the monthly (or even daily) N fertilizer loadings in the global scale. Because the N fertilizer data underlying the gridded products is derived from the annual statistics by the Food and Agricultural Organization (FAO) (https://www.fao.org/faostat/en/#data), the HaNi dataset applied this study, as well as the equivalently up-to-date fertilizer dataset (Adalibieke et al., 2023), only provides gridded, annual fertilizer application rates. In the EF approaches, the growing season is determined only by temperature and greenness in this study, which could result in a mismatch with the real crop or pasture calendar, especially ignoring the multiple-harvest crops per year. A refined calendar could further improve the prediction of SNO_x-Fer seasonality. Furthermore, the NO_x-VOCs-O₃ chemical sensitivity regimes could be determined by not only soil NO_x emissions, but also other anthropogenic and biogenic emissions of NO_x and VOCs, as well as the climate seasonal variations. Therefore, the seasonal cycles of the enhancement of O₃ concentrations may not strictly follow the variations in SNO_x-Fer, as our Linear 75 sensitivity experiment implies in Western Europe and Eastern Asia (Figs. 5b and 5c). The impacts of the changes in short-lived air pollutants on global CH₄ budget have attracted increasing attention in recent years (Peng et al., 2022; Zhao et al., 2025), where NO_x is one of the most important drivers. However, it should be noted that the sensitivity of CH₄ lifetime to NO_x emissions varies substantially among atmospheric chemistry models from -25% to -46% in response to the total NO_x changes from pre-industrial to present-day period (Thornhill et al., 2021). Because few studies investigated how NO_x from agricultural sources affects CH₄, it is difficult to assess if the overall impacts of SNO_x-Fer on CH₄ presented in this study based on the GEOS-Chem model are underestimated or

415

416

417

418

419

420

421

422

423

424

425

426

427

428

429

430

431

432

433

434

435

436

437

438

439

440

441

442443

444

445

446

447

448

449

overestimated, even though certain uncertainties are expected. Nevertheless, our results indicate that SNO_x -Fer could be one uncertain but important source in calculating future changes of the global CH_4 budget, the importance of which could be increasing with future continuing reduction in fossil-fuel NO_x emissions (Rao et al., 2017)

451

452

453

454

455

456

457

458

459

460

461

462

463

464

465

466

467

468

469

470

471

472

473

474

475

476

477

478

479

480

481

482

483

484

485

486

Beyond the uncertainties remaining in different SNO_x-Fer estimating approaches, an important but also difficult question is how to better evaluate the performances of each methods, especially in the regional and global scales. The first-hand meta-data collected from the field experiments is actually not an independent source, as it has been used to establish both of the linear and nonlinear EF methods. More importantly, most of the field experiments are manipulation experiments with artificial fertilizer gradients, which may not fully represent the real-world spatiotemporally varied SNO_x-Fer. Furthermore, we use O_3 data from the national or continental air quality observational networks to evaluate simulated O₃ concentrations as a potential consistency check of the SNO_x-Fer (Fig. S7). However, the uncertainties in SNO_x-Fer are expected to be far less important relative to the uncertainties in the nonlinearity of atmospheric chemistry, emissions of BVOCs or the deposition processes, which together determined the biases between observational and simulated O₃ concentrations. As a result, it is inappropriate to determine the best SNO_x-Fer estimate as the one with the best statistic metrics in O₃ simulation. Moreover, most of the sites that monitoring air pollutants are located in the urban regions, where the industrial impacts are far more important than the agricultural sources. A real-time O₃ observational network in the cropland or pasture would be crucial to advance the understandings in SNO_x-Fer and the associated impacts on air quality. Last but not least, the top-down retrievals of NO_x emissions based on satellite NO₂ products could also have the potential to better constrain SNO_x-Fer, while gaps remained in how to precisely isolate the soil NO_x emissions (Bertram et al., 2005; Lin et al., 2024) and even the fertilizer contributions from the total NO_x sources. Synergizing spatiotemporally detailed fertilizer management dataset with the top-down NO_x retrievals with ultra-high resolutions, where the atmospheric NO_x can be assumed to be dominantly affected by the soil sources in agricultural regions, could be one possible solution. However, more work is needed to integrate such a big data in the future.

To summarize, with a comprehensive investigation of different approaches to describe SNO_x-Fer, our results revealed the uncertainties in quantifying SNO_x-Fer and associated important implications in simulating regional air quality and the global greenhouse gas CH₄. However, the limited number of field experiments impedes accurate assessments of the soil NO_x responses to N fertilizer application as well as improving its representation in both CTMs and TBMs, resulting in large uncertainties in estimates of N fertilizer-induced soil NO_x emissions. We thus highlight the essential necessity to integrate knowledge between agricultural data, atmospheric chemistry modelling and soil biogeochemistry to better represent soil NO_x emissions in models and improve our understanding of the associated effects on air quality and the global CH₄ budget.

488	Acknowledgement
489	C.G. and S.Z. acknowledge support from the European Commission H2020 programme (Grant-No.
490	101003536; ESM2025).
491	
492	Code and data availability
493	The GEOS-Chem source code can be assessed in https://github.com/geoschem/geos-chem . The CEDS
494	inventory used in GEOS-Chem can be downloaded at
495	https://ftp.as.harvard.edu/gcgrid/data/ExtData/HEMCO/CEDS/. The NMIP2 model outputs can be
496	downloaded through the open-accessed data in Gong et al. (2024).
497	
400	Author contributions
498	Author contributions
499	C.G. designed the study. C.G. performed the GEOS-Chem simulations and data analysis. Y.W. helps
500	the non-linear EF analysis. H.T. led the NMIP2 projects. S.K, N.V., and S.Z. together contributed to
501	the simulation of terrestrial biosphere models in NMIP2. C.G. wrote the manuscript. All of the authors
502	contributed to reviewing or editing the manuscript.
503	
504	Conflict of interest
505	The authors declare no conflict of interest.
506	
507	References:
508	Adalibieke, W., Cui, X. Q., Cai, H. W., You, L. Z., and Zhou, F.: Global crop-specific nitrogen
509	fertilization dataset in 1961-2020, Scientific Data, 10, 10.1038/s41597-023-02526-z, 2023.
510	Bates, K. H., Evans, M. J., Henderson, B. H., and Jacob, D. J.: Impacts of updated reaction kinetics on
511	the global GEOS-Chem simulation of atmospheric chemistry, Geoscientific Model Development, 17,
512	1511-1524, 10.5194/gmd-17-1511-2024, 2024. Rottram T. H. Hackel, A. Richter, A. Burrows, J. B. and Cohen, R. C. Satellita massuraments of
513 514	Bertram, T. H., Heckel, A., Richter, A., Burrows, J. P., and Cohen, R. C.: Satellite measurements of daily variations in soil NOx emissions -: art. no. L24812, Geophysical Research Letters, 32,
515	10.1029/2005gl024640, 2005.
516	Bey, I., Jacob, D. J., Yantosca, R. M., Logan, J. A., Field, B. D., Fiore, A. M., Li, Q. B., Liu, H. G. Y.,
517	Mickley, L. J., and Schultz, M. G.: Global modeling of tropospheric chemistry with assimilated
518	meteorology: Model description and evaluation, Journal of Geophysical Research-Atmospheres, 106,
519	23073-23095, 10.1029/2001jd000807, 2001.

- 520 Cheng, W. G., Tsuruta, H., Chen, G. X., and Yagi, K.: N2O and NO production in various Chinese
- agricultural soils by nitrification, Soil Biology & Biochemistry, 36, 953-963,
- 522 10.1016/j.soilbio.2004.02.012, 2004.
- 523 Delmas, R., Serca, D., and Jambert, C.: Global inventory of NOx sources, Nutrient Cycling in
- 524 Agroecosystems, 48, 51-60, 10.1023/a:1009793806086, 1997.
- 525 Du, E. Z. and de Vries, W.: Links Between Nitrogen Limitation and Saturation in Terrestrial
- 526 Ecosystems, Global Change Biology, 31, 10.1111/gcb.70271, 2025.
- East, J. D., Jacob, D. J., Balasus, N., Bloom, A. A., Bruhwiler, L., Chen, Z. C., Kaplan, J. O., Mickley, L. J.,
- Mooring, T. A., Penn, E., Poulter, B., Sulprizio, M. P., Worden, J. R., Yantosca, R. M., and Zhang, Z.:
- 529 Interpreting the Seasonality of Atmospheric Methane, Geophysical Research Letters, 51,
- 530 10.1029/2024gl108494, 2024.
- 531 Eggleston, H., Buendia, L., Miwa, K., Ngara, T., and Tanabe, K.: 2006 IPCC guidelines for national
- 532 greenhouse gas inventories, 2006.
- 533 Erisman, J. W., Galloway, J., Seitzinger, S., Bleeker, A., and Butterbach-Bahl, K.: Reactive nitrogen in
- the environment and its effect on climate change, Current Opinion in Environmental Sustainability,
- 535 3, 281-290, 10.1016/j.cosust.2011.08.012, 2011.
- Fleischer, K., Dolman, A. J., van der Molen, M. K., Rebel, K. T., Erisman, J. W., Wassen, M. J., Pak, B.,
- 537 Lu, X. J., Rammig, A., and Wang, Y. P.: Nitrogen Deposition Maintains a Positive Effect on Terrestrial
- 538 Carbon Sequestration in the 21st Century Despite Growing Phosphorus Limitation at Regional Scales,
- 539 Global Biogeochemical Cycles, 33, 810-824, 10.1029/2018gb005952, 2019.
- 540 Fountoukis, C. and Nenes, A.: ISORROPIA II: a computationally efficient thermodynamic equilibrium
- model for K+-Ca2+-Mg2+-Nh(4)(+)-Na+-SO42--NO3--Cl--H2O aerosols, Atmospheric Chemistry and
- 542 Physics, 7, 4639-4659, 10.5194/acp-7-4639-2007, 2007.
- Fowler, D., Coyle, M., Skiba, U., Sutton, M. A., Cape, J. N., Reis, S., Sheppard, L. J., Jenkins, A.,
- 544 Grizzetti, B., Galloway, J. N., Vitousek, P., Leach, A., Bouwman, A. F., Butterbach-Bahl, K., Dentener,
- 545 F., Stevenson, D., Amann, M., and Voss, M.: The global nitrogen cycle in the twenty-first century,
- Philosophical Transactions of the Royal Society B-Biological Sciences, 368, 10.1098/rstb.2013.0164,
- 547 2013
- 548 Fu, B., Li, J. Y., Jiang, Y. Y., Chen, Z. W., and Li, B. A.: Clean air policy makes methane harder to control
- due to longer lifetime, One Earth, 7, 10.1016/j.oneear.2024.06.010, 2024.
- 550 Goldberg, D. L., Harkey, M., de Foy, B., Judd, L., Johnson, J., Yarwood, G., and Holloway, T.:
- 551 Evaluating NOx emissions and their effect on O3 production in Texas using TROPOMI NO2 and
- 552 HCHO, Atmospheric Chemistry and Physics, 22, 10875-10900, 10.5194/acp-22-10875-2022, 2022.
- Gong, C., Liao, H., Zhang, L., Yue, X., Dang, R. J., and Yang, Y.: Persistent ozone pollution episodes in
- North China exacerbated by regional transport, Environmental Pollution, 265,
- 555 10.1016/j.envpol.2020.115056, 2020.
- 556 Gong, C., Tian, H., Liao, H., Pan, N., Pan, S., Ito, A., Jain, A. K., Kou-Giesbrecht, S., Joos, F., Sun, Q., Shi,
- 557 H., Vuichard, N., Zhu, Q., Peng, C., Maggi, F., Tang, F. H. M., and Zaehle, S.: Global net climate effects
- of anthropogenic reactive nitrogen, Nature, 10.1038/s41586-024-07714-4, 2024.
- Henze, D. K., Hakami, A., and Seinfeld, J. H.: Development of the adjoint of GEOS-Chem, Atmospheric
- 560 Chemistry and Physics, 7, 2413-2433, 10.5194/acp-7-2413-2007, 2007.
- Hergoualc'h, K., Akiyama, H., Bernoux, M., Chirinda, N., Prado, A. d., Kasimir, Å., MacDonald, J. D.,
- 562 Ogle, S. M., Regina, K., and Weerden, T. J. v. d.: N2O emissions from managed soils, and CO2
- 563 emissions from lime and urea application, 2019.
- Hoesly, R. M., Smith, S. J., Feng, L. Y., Klimont, Z., Janssens-Maenhout, G., Pitkanen, T., Seibert, J. J.,
- Vu, L., Andres, R. J., Bolt, R. M., Bond, T. C., Dawidowski, L., Kholod, N., Kurokawa, J., Li, M., Liu, L.,
- 566 Lu, Z. F., Moura, M. C. P., O'Rourke, P. R., and Zhang, Q.: Historical (1750-2014) anthropogenic
- 567 emissions of reactive gases and aerosols from the Community Emissions Data System (CEDS),
- 568 Geoscientific Model Development, 11, 369-408, 10.5194/gmd-11-369-2018, 2018.
- Huber, D. E., Steiner, A. L., and Kort, E. A.: Sensitivity of Modeled Soil NOx Emissions to Soil Moisture,
- Journal of Geophysical Research-Atmospheres, 128, 10.1029/2022jd037611, 2023.

- Hudman, R. C., Moore, N. E., Mebust, A. K., Martin, R. V., Russell, A. R., Valin, L. C., and Cohen, R. C.:
- 572 Steps towards a mechanistic model of global soil nitric oxide emissions: implementation and space
- 573 based-constraints, Atmospheric Chemistry and Physics, 12, 7779-7795, 10.5194/acp-12-7779-2012,
- 574 2012.
- 575 Hurtt, G. C., Chini, L., Sahajpal, R., Frolking, S., Bodirsky, B. L., Calvin, K., Doelman, J. C., Fisk, J.,
- 576 Fujimori, S., Goldewijk, K. K., Hasegawa, T., Havlik, P., Heinimann, A., Humpenoder, F., Jungclaus, J.,
- 577 Kaplan, J. O., Kennedy, J., Krisztin, T., Lawrence, D., Lawrence, P., Ma, L., Mertz, O., Pongratz, J.,
- 578 Popp, A., Poulter, B., Riahi, K., Shevliakova, E., Stehfest, E., Thornton, P., Tubiello, F. N., van Vuuren,
- 579 D. P., and Zhang, X.: Harmonization of global land use change and management for the period 850-
- 580 2100 (LUH2) for CMIP6, Geoscientific Model Development, 13, 5425-5464, 10.5194/gmd-13-5425-
- 581 2020, 2020.
- 582 Janssens-Maenhout, G., Crippa, M., Guizzardi, D., Muntean, M., Schaaf, E., Dentener, F.,
- Bergamaschi, P., Pagliari, V., Olivier, J. G. J., Peters, J., van Aardenne, J. A., Monni, S., Doering, U.,
- 584 Petrescu, A. M. R., Solazzo, E., and Oreggioni, G. D.: EDGAR v4.3.2 Global Atlas of the three major
- 585 greenhouse gas emissions for the period 1970-2012, Earth System Science Data, 11, 959-1002,
- 586 10.5194/essd-11-959-2019, 2019.
- 587 Jiang, Y., Deng, A. X., Bloszies, S., Huang, S., and Zhang, W. J.: Nonlinear response of soil ammonia
- emissions to fertilizer nitrogen, Biology and Fertility of Soils, 53, 269-274, 10.1007/s00374-017-1175-
- 589 3, 2017.
- 590 Jiang, Z., Zhu, R., Miyazaki, K., McDonald, B. C., Klimont, Z., Zheng, B., Boersma, K. F., Zhang, Q.,
- Worden, H., Worden, J. R., Henze, D. K., Jones, D. B. A., van der Gon, H., and Eskes, H.: Decadal
- Variabilities in Tropospheric Nitrogen Oxides Over United States, Europe, and China, Journal of
- 593 Geophysical Research-Atmospheres, 127, 10.1029/2021jd035872, 2022.
- 594 Kou-Giesbrecht, S., Arora, V. K., Seiler, C., Arneth, A., Falk, S., Jain, A. K., Joos, F., Kennedy, D.,
- 595 Knauer, J., Sitch, S., O'Sullivan, M., Pan, N., Sun, Q., Tian, H., Vuichard, N., and Zaehle, S.: Evaluating
- 596 nitrogen cycling in terrestrial biosphere models: a disconnect between the carbon and nitrogen
- 597 cycles, Earth Syst. Dynam., 14, 767-795, 10.5194/esd-14-767-2023, 2023.
- 598 Lin, X. J., Ronald, V., de Laat, J., Huijnen, V., Mijling, B., Ding, J. Y., Eskes, H., Douros, J., Liu, M. Y.,
- 599 Zhang, X., and Liu, Z.: European Soil NOx Emissions Derived From Satellite NO2 Observations, Journal
- of Geophysical Research-Atmospheres, 129, 10.1029/2024jd041492, 2024.
- 601 Liu, S. W., Lin, F., Wu, S., Ji, C., Sun, Y., Jin, Y. G., Li, S. Q., Li, Z. F., and Zou, J. W.: A meta-analysis of
- 602 fertilizer-induced soil NO and combined NO+N₂O emissions, Global Change Biology, 23,
- 603 2520-2532, 10.1111/gcb.13485, 2017.
- 604 Lu, X., Ye, X. P., Zhou, M., Zhao, Y. H., Weng, H. J., Kong, H., Li, K., Gao, M., Zheng, B., Lin, J. T., Zhou,
- 605 F., Zhang, Q., Wu, D. M., Zhang, L., and Zhang, Y. H.: The underappreciated role of agricultural soil
- nitrogen oxide emissions in ozone pollution regulation in North China, Nature Communications, 12,
- 607 10.1038/s41467-021-25147-9, 2021.
- 608 Martin, R. V., Jacob, D. J., Chance, K., Kurosu, T. P., Palmer, P. I., and Evans, M. J.: Global inventory of
- 609 nitrogen oxide emissions constrained by space-based observations of NO₂ columns -:
- art. no. 4537, Journal of Geophysical Research-Atmospheres, 108, 10.1029/2003jd003453, 2003.
- 611 Matson, P. A., Naylor, R., and Ortiz-Monasterio, I.: Integration of environmental, agronomic, and
- 612 economic aspects of fertilizer management, Science, 280, 112-115, 10.1126/science.280.5360.112,
- 613 1998.
- Nicholas Hutchings, J. Webb, and Amon, B.: EMEP/EEA air pollutant emission inventory guidebook
- 615 2023: 3.D Agricultural soils 2023, 2023.
- Park, R. J., Jacob, D. J., Field, B. D., Yantosca, R. M., and Chin, M.: Natural and transboundary
- 617 pollution influences on sulfate-nitrate-ammonium aerosols in the United States: Implications for
- 618 policy, Journal of Geophysical Research-Atmospheres, 109, 10.1029/2003jd004473, 2004.
- 619 Peng, S. S., Lin, X., Thompson, R. L., Xi, Y., Liu, G., Hauglustaine, D., Lan, X., Poulter, B., Ramonet, M.,
- 620 Saunois, M., Yin, Y., Zhang, Z., Zheng, B., and Ciais, P.: Wetland emission and atmospheric sink
- 621 changes explain methane growth in 2020, Nature, 612, 477-+, 10.1038/s41586-022-05447-w, 2022.

- 622 Pinder, R. W., Davidson, E. A., Goodale, C. L., Greaver, T. L., Herrick, J. D., and Liu, L. L.: Climate
- 623 change impacts of US reactive nitrogen, Proceedings of the National Academy of Sciences of the
- 624 United States of America, 109, 7671-7675, 10.1073/pnas.1114243109, 2012.
- 625 Rao, S., Klimont, Z., Smith, S. J., Van Dingenen, R., Dentener, F., Bouwman, L., Riahi, K., Amann, M.,
- 626 Bodirsky, B. L., van Vuuren, D. P., Reis, L. A., Calvin, K., Drouet, L., Fricko, O., Fujimori, S., Gernaat, D.,
- 627 Havlik, P., Harmsen, M., Hasegawa, T., Heyes, C., Hilaire, J., Luderer, G., Masui, T., Stehfest, E.,
- 628 Strefler, J., van der Sluis, S., and Tavoni, M.: Future air pollution in the Shared Socio-economic
- 629 Pathways, Global Environmental Change-Human and Policy Dimensions, 42, 346-358,
- 630 10.1016/j.gloenvcha.2016.05.012, 2017.
- 631 Rubin, H. J., Fu, J. S., Dentener, F., Li, R., Huang, K., and Fu, H. B.: Global nitrogen and sulfur
- deposition mapping using a measurement-model fusion approach, Atmospheric Chemistry and
- 633 Physics, 23, 7091-7102, 10.5194/acp-23-7091-2023, 2023.
- Russell, A. R., Perring, A. E., Valin, L. C., Bucsela, E. J., Browne, E. C., Min, K. E., Wooldridge, P. J., and
- 635 Cohen, R. C.: A high spatial resolution retrieval of NO₂ column densities from OMI:
- method and evaluation, Atmospheric Chemistry and Physics, 11, 8543-8554, 10.5194/acp-11-8543-
- 637 2011, 2011.
- 638 Shcherbak, I., Millar, N., and Robertson, G. P.: Global metaanalysis of the nonlinear response of soil
- 639 nitrous oxide (N2O) emissions to fertilizer nitrogen, Proceedings of the National Academy of
- 640 Sciences of the United States of America, 111, 9199-9204, 10.1073/pnas.1322434111, 2014.
- 641 Skiba, U., Medinets, S., Cardenas, L. M., Carnell, E. J., Hutchings, N., and Amon, B.: Assessing the
- contribution of soil NO<i><sub></i> emissions to European atmospheric pollution,
- 643 Environmental Research Letters, 16, 10.1088/1748-9326/abd2f2, 2021.
- 644 Stehfest, E. and Bouwman, L.: N2O and NO emission from agricultural fields and soils under natural
- vegetation:: summarizing available measurement data and modeling of global annual emissions,
- 646 Nutrient Cycling in Agroecosystems, 74, 207-228, 10.1007/s10705-006-9000-7, 2006.
- 647 Steinkamp, J. and Lawrence, M. G.: Improvement and evaluation of simulated global biogenic soil NO
- emissions in an AC-GCM, Atmospheric Chemistry and Physics, 11, 6063-6082, 10.5194/acp-11-6063-
- 649 2011, 2011
- Thornhill, G. D., Collins, W. J., Kramer, R. J., Olivi, D., Skeie, R. B., O'Connor, F. M., Abraham, N. L.,
- 651 Checa-Garcia, R., Bauer, S. E., Deushi, M., Emmons, L. K., Forster, P. M., Horowitz, L. W., Johnson, B.,
- 652 Keeble, J., Lamarque, J. F., Michou, M., Mills, M. J., Mulcahy, J. P., Myhre, G., Nabat, P., Naik, V.,
- 653 Oshima, N., Schulz, M., Smith, C. J., Takemura, T., Tilmes, S., Wu, T. W., Zeng, G., and Zhang, J.:
- 654 Effective radiative forcing from emissions of reactive gases and aerosols a multi-model comparison,
- Atmospheric Chemistry and Physics, 21, 853-874, 10.5194/acp-21-853-2021, 2021.
- 656 Tian, H., Pan, N., Thompson, R. L., Canadell, J. G., Suntharalingam, P., Regnier, P., Davidson, E. A.,
- 657 Prather, M., Ciais, P., Muntean, M., Pan, S., Winiwarter, W., Zaehle, S., Zhou, F., Jackson, R. B.,
- 658 Bange, H. W., Berthet, S., Bian, Z., Bianchi, D., Bouwman, A. F., Buitenhuis, E. T., Dutton, G., Hu, M.,
- 659 Ito, A., Jain, A. K., Jeltsch-Thömmes, A., Joos, F., Kou-Giesbrecht, S., Krummel, P. B., Lan, X., Landolfi,
- 660 A., Lauerwald, R., Li, Y., Lu, C., Maavara, T., Manizza, M., Millet, D. B., Mühle, J., Patra, P. K., Peters,
- 661 G. P., Qin, X., Raymond, P., Resplandy, L., Rosentreter, J. A., Shi, H., Sun, Q., Tonina, D., Tubiello, F.
- 662 N., van der Werf, G. R., Vuichard, N., Wang, J., Wells, K. C., Western, L. M., Wilson, C., Yang, J., Yao,
- 663 Y., You, Y., and Zhu, Q.: Global nitrous oxide budget (1980–2020), Earth Syst. Sci. Data, 16, 2543-
- 664 2604, 10.5194/essd-16-2543-2024, 2024.
- Tian, H. Q., Bian, Z. H., Shi, H., Qin, X. Y., Pan, N. Q., Lu, C. Q., Pan, S. F., Tubiello, F. N., Chang, J. F.,
- 666 Conchedda, G., Liu, J. G., Mueller, N., Nishina, K., Xu, R. T., Yang, J., You, L. Z., and Zhang, B. W.:
- History of anthropogenic Nitrogen inputs (HaNi) to the terrestrial biosphere: a 5 arcmin resolution
- annual dataset from 1860 to 2019, Earth System Science Data, 14, 4551-4568, 10.5194/essd-14-
- 669 4551-2022, 2022
- 670 Tian, H. Q., Yang, J., Xu, R. T., Lu, C. Q., Canadell, J. G., Davidson, E. A., Jackson, R. B., Arneth, A.,
- 671 Chang, J. F., Ciais, P., Gerber, S., Ito, A., Joos, F., Lienert, S., Messina, P., Olin, S., Pan, S. F., Peng, C.
- 672 H., Saikawa, E., Thompson, R. L., Vuichard, N., Winiwarter, W., Zaehle, S., and Zhang, B. W.: Global

- 673 soil nitrous oxide emissions since the preindustrial era estimated by an ensemble of terrestrial
- 674 biosphere models: Magnitude, attribution, and uncertainty, Global Change Biology, 25, 640-659,
- 675 10.1111/gcb.14514, 2019.
- 676 Wang, Y., Yao, Z. S., Zheng, X. H., Subramaniam, L., and Butterbach-Bahl, K.: A synthesis of nitric
- 677 oxide emissions across global fertilized croplands from crop-specific emission factors, Global Change
- 678 Biology, 28, 4395-4408, 10.1111/gcb.16193, 2022.
- 679 Wang, Y., Ge, C., Garcia, L. C., Jenerette, G. D., Oikawa, P. Y., and Wang, J.: Improved modelling of
- soil NOx emissions in a high temperature agricultural region: role of background emissions on NO2
- trend over the US, Environmental Research Letters, 16, 10.1088/1748-9326/ac16a3, 2021.
- 682 Wang, Y., Yao, Z. S., Pan, Z. L., Guo, H. J., Chen, Y. C., Cai, Y. J., and Zheng, X. H.: Nonlinear response
- of soil nitric oxide emissions to fertilizer nitrogen across croplands, Biology and Fertility of Soils, 60,
- 684 483-492, 10.1007/s00374-024-01818-9, 2024.
- 685 Weng, H. J., Lin, J. T., Martin, R., Millet, D. B., Jaegle, L., Ridley, D., Keller, C., Li, C., Du, M. X., and
- 686 Meng, J.: Global high-resolution emissions of soil NOx, sea salt aerosols, and biogenic volatile organic
- 687 compounds, Scientific Data, 7, 10.1038/s41597-020-0488-5, 2020.
- 688 Yienger, J. J. and Levy, H.: EMPIRICAL-MODEL OF GLOBAL SOIL-BIOGENIC NOX EMISSIONS, Journal of
- 689 Geophysical Research-Atmospheres, 100, 11447-11464, 10.1029/95jd00370, 1995.
- 690 Yuan, H., Dai, Y. J., Xiao, Z. Q., Ji, D. Y., and Shangguan, W.: Reprocessing the MODIS Leaf Area Index
- 691 products for land surface and climate modelling, Remote Sensing of Environment, 115, 1171-1187,
- 692 10.1016/j.rse.2011.01.001, 2011.
- 693 Zaehle, S. and Dalmonech, D.: Carbon-nitrogen interactions on land at global scales: current
- 694 understanding in modelling climate biosphere feedbacks, Current Opinion in Environmental
- 695 Sustainability, 3, 311-320, 10.1016/j.cosust.2011.08.008, 2011.
- 696 Zaehle, S. and Friend, A. D.: Carbon and nitrogen cycle dynamics in the O-CN land surface model: 1.
- 697 Model description, site-scale evaluation, and sensitivity to parameter estimates, Global
- 698 Biogeochemical Cycles, 24, 10.1029/2009gb003521, 2010.
- 699 Zhai, S. X., Jacob, D. J., Wang, X., Liu, Z. R., Wen, T. X., Shah, V., Li, K., Moch, J. M., Bates, K. H., Song,
- 700 S. J., Shen, L., Zhang, Y. Z., Luo, G., Yu, F. Q., Sun, Y. L., Wang, L. T., Qi, M. Y., Tao, J., Gui, K., Xu, H. H.,
- 701 Zhang, Q., Zhao, T. L., Wang, Y. S., Lee, H. C., Choi, H., and Liao, H.: Control of particulate nitrate air
- 702 pollution in China, Nature Geoscience, 14, 389-+, 10.1038/s41561-021-00726-z, 2021.
- 703 Zhang, R. Y., Tie, X. X., and Bond, D. W.: Impacts of anthropogenic and natural NO_x
- 704 sources over the US on tropospheric chemistry, Proceedings of the National Academy of Sciences of
- 705 the United States of America, 100, 1505-1509, 10.1073/pnas.252763799, 2003.
- 706 Zhao, Y., Saunois, M., Bousquet, P., Lin, X., Hegglin, M. I., Canadell, J. G., Jackson, R. B., and Zheng, B.:
- 707 Reconciling the bottom-up and top-down estimates of the methane chemical sink using multiple
- 708 observations, Atmos. Chem. Phys., 23, 789-807, 10.5194/acp-23-789-2023, 2023.
- 709 Zhao, Y. H., Zheng, B., Saunois, M., Ciais, P., Hegglin, M. I., Lu, S. M., Li, Y. F., and Bousquet, P.: Air
- 710 pollution modulates trends and variability of the global methane budget, Nature, 642,
- 711 10.1038/s41586-025-09004-z, 2025.